

# Quantum measurement characteristics of double-dot single electron transistor

HuJun Jiao\* and Xin-Qi Li†

State Key Laboratory for Superlattices and Microstructures, Institute of Semiconductors,  
Chinese Academy of Sciences, P.O. Box 912, Beijing 100083, China

JunYan Luo

State Key Laboratory for Superlattices and Microstructures, Institute of Semiconductors,  
Chinese Academy of Sciences, P.O. Box 912, Beijing 100083, China and  
Department of Chemistry, Hong Kong University of Science and Technology, Kowloon, Hong Kong  
(Dated: March 1, 2019)

Owing to a few unique advantages, double-dot single electron transistor has been proposed as an alternative detector for charge states. In this work, we present a further study for its signal-to-noise property, based on a full analysis of the setup configuration symmetry. It is found that the effectiveness of the double-dot detector can approach that of an ideal detector, if the symmetric capacitive coupling is taken into account. The quantum measurement efficiency is also analyzed, by comparing the measurement time with the measurement-induced dephasing time.

Quantum measurement in solid-state mesoscopic systems has attracted considerable interest in the past years [1, 2, 3, 4, 5, 6, 7]. Besides the intensive theoretical work, experimental progresses are in particular impressive [8, 9, 10, 11, 12, 13, 14, 15]. In these studies, two measurement devices were typically focused on, i.e., the mesoscopic quantum point contact (QPC) and the single electron transistor (SET). Usually, the SET is restricted to the device with a single dot embedded in between the source and drain electrodes. Very recently, the double-dot (DD) SET has been proposed as an alternative charge detector [16, 17, 18, 19, 20, 21]. Compared to the single-dot detector, in addition to the obvious advantage of weakening the requirement of very low temperature, the DD detector may have other advantages such as: (i) It can probe the rapid transitions between electrostatically degenerate charge states [17]. Experimentally, its radio-frequency operation has been demonstrated [18]. (ii) DD detector is able to probe the entanglement of two qubits [19]. (iii) Most importantly, DD detector has better immunity against noises [20].

Owing to the added complexity of the DD detector, better understanding of its measurement dynamics is of interest and seems a timely work at this stage. Very recently, this problem was studied by Gilad and Gurvitz [21]. The key insight gained in their work is the *symmetry* property of the setup configuration, which is revealed in terms of the response current of the DD detector in both the time and frequency domains. However, their analysis was based on an *extremely asymmetric* capacitive coupling configuration, which leads to a conclusion that the DD detector is a sensitive detector, but *cannot* reach the signal-to-noise ratio of 4, i.e., the value of an ideal QPC detector.

In this work, we present a further study for the signal-

to-noise property of the DD detector, based on a full analysis of the capacitive coupling symmetry. In contrast with Ref. 21, we conclude that the DD detector can approach the signal-to-noise ratio of an ideal QPC detector, if the symmetric capacitive coupling setup is taken into account. Moreover, we also analyze the *quantum measurement efficiency* of the DD detector, by comparing the measurement time with the measurement-induced dephasing time. It is found that, under the setup configuration that results in the optimal signal-to-noise ratio, the measurement efficiency cannot reach unity (i.e. the value of ideal QPC detector). However, in principle, it can approach unity under proper parametric conditions.

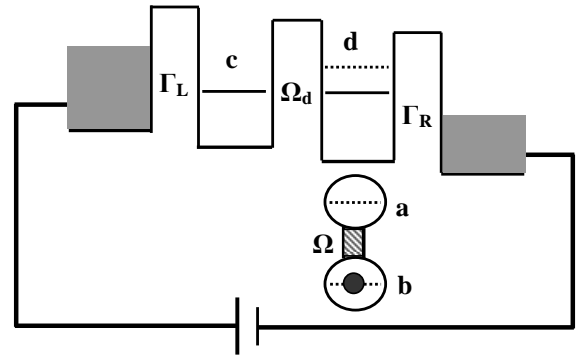


FIG. 1: Schematic setup of using the double-dot single electron transistor to perform quantum measurement of a solid-state qubit.

## Model Description

As schematically shown in Fig.1, let us consider a charge qubit measured by a mesoscopic transport device. The charge qubit studied here is modeled by a pair of coupled quantum dots with an extra electron in it, while

\*Electronic address: jiaohujun@semi.ac.cn

†Electronic address: xqli@red.semi.ac.cn

the detector is the proposed DD single electron transistor. The entire system is described by the following Hamiltonian

$$H = H_0 + H' \quad (1a)$$

$$H_0 = H_s + \sum_k (\epsilon_k^L c_k^\dagger c_k + \epsilon_k^R d_k^\dagger d_k) \quad (1b)$$

$$H_s = \sum_{i=a,b,c,d} E_i a_i^\dagger a_i + \Omega(a_a^\dagger a_b + a_b^\dagger a_a) + \Omega_d(a_c^\dagger a_d + a_d^\dagger a_c) + \sum_{i=a,b} \sum_{j=c,d} U_{ij} n_i n_j + U_{cd} n_c n_d \quad (1c)$$

$$H' = \sum_k (\Omega_k^L a_c^\dagger c_k + \Omega_k^R a_d^\dagger d_k + \text{H.c.}) \equiv a_c^\dagger f_c + a_d^\dagger f_d + \text{H.c.} \quad (1d)$$

In these decomposed Hamiltonians,  $a_a^\dagger(a_a)$ ,  $a_b^\dagger(a_b)$ ,  $a_c^\dagger(a_c)$ ,  $a_d^\dagger(a_d)$ ,  $c_k^\dagger(c_k)$  and  $d_k^\dagger(d_k)$  are the electron creation (annihilation) operators of the qubit, detector's two central dots and the reservoirs. In the following treatment, the tunneling Hamiltonian  $H'$  of the DD detector will be taken as perturbation. The free Hamiltonian in the above,  $H_0$ , consists of the detector's reservoirs, its central two dots, the qubit, and the Coulomb interaction between them.

In this work, we assume that the DD detector works in the strong Coulomb-blockade regime, i.e., there will be at most one more electron occupied in the two dots. Therefore, only the three DD states  $|00\rangle$ ,  $|10\rangle$ , and  $|01\rangle$  are involved in the transport process. Here, 0 and 1 stand for the vacant and occupied dot states, while their ordering in  $|\dots\rangle$  is from the left to the right dot states of the detector. For the qubit, it has two logic states, i.e., the dot states  $|a\rangle$  and  $|b\rangle$ . For the sake of simplicity, we assume that each dot has only one bound state. Intuitively, the measurement principle of the device under study is as follows: if the qubit is in state  $|b\rangle$ , the two states  $|10\rangle$  and  $|01\rangle$  of the DD detector is nearly energetically degenerate; while the qubit is in state  $|a\rangle$ , they will be in off-resonance, due to the relatively stronger Coulomb interaction  $U_{ad}$ . Accordingly, the resultant different output currents of the DD detector can distinguish the qubit states.

### “ $n$ ”-Resolved Master Equation

In the reduced description, the central dots of the detector and the qubit are the *system of interest*, and the two reservoirs of the detector are the *environment*. The first step is to derive a master equation for the system of interest. Moreover, in order to relate the master equation also to the output of the detector, one should obtain a “ $n$ ”-resolved master equation. Here, “ $n$ ” denotes the number of electrons in certain specified time interval that have tunneled through the left or right junction of the transport device. Following the work by Li *et al* [22, 23],

we obtain

$$\begin{aligned} \dot{\rho}^{(n_R)} = & -i\mathcal{L}\rho^{(n_R)} - \frac{1}{2}\{[a_c^\dagger, A_c^{(-)}\rho^{(n_R)} - \rho^{(n_R)}A_c^{(+)}] \\ & + a_d^\dagger A_d^{(-)}\rho^{(n_R)} + \rho^{(n_R)}A_d^{(+)}a_d^\dagger \\ & - [a_d^\dagger\rho^{(n_R+1)}A_d^{(+)} + A_d^{(-)}\rho^{(n_R-1)}a_d^\dagger] + \text{H.c.}\}. \end{aligned} \quad (2)$$

Note that throughout this paper we shall use the unit system of  $\hbar = e = k_B = 1$ . Shown above is in fact the “ $n_R$ ”-resolved master equation, with “ $n_R$ ” the number of electrons tunneled through the right junction. Similar equation can be carried out for the left-junction specified tunneled electrons. The superoperators in Eq. (2) read  $A_\alpha^{(\pm)} = C_\alpha^{(\pm)}(\pm\mathcal{L})a_\alpha$ .  $C_\alpha^{(\pm)}(\pm\mathcal{L})$  are the spectral functions of the two reservoirs, which are the Fourier transform of the correlation functions, i.e.,  $C_\alpha^{(\pm)}(\pm\mathcal{L}) = \int_{-\infty}^{+\infty} dt C_\alpha^{(\pm)}(t)e^{\pm i\mathcal{L}t}$ , with  $C_\alpha^{(+)}(t) = \langle f_\alpha^\dagger(t)f_\alpha \rangle$  and  $C_\alpha^{(-)}(t) = \langle f_\alpha(t)f_\alpha^\dagger \rangle$ .

Note that the Liouvillian  $\mathcal{L}$  is defined by  $\mathcal{L}(\dots) = [H_S, \dots]$ . To explicitly carry out the action of its arbitrary function on an operator (e.g.  $a_c$  or  $a_d$ ), a convenient way is doing it in the eigenstate basis of  $H_S$ . In this basis, the matrix element of the arbitrary function of  $\mathcal{L}$  is obtained by simply replacing  $\mathcal{L}$  with the energy difference of the two basis states.

### Readout Characteristics

Note that  $\rho^{(n)}$  contains rich information about the measurement. From it, one can obtain the distribution function of the tunneled electron numbers, the output current and the noise spectrum. Quite clearly, the distribution function reads  $P(n_R, t) = \text{Tr}[\rho^{n_R}(t)]$ , where the trace is over the states of the system of interest. Then, the current through the right junction is

$$\begin{aligned} I_R(t) = & \sum_{n_R} \text{Tr}\{n_R \dot{\rho}^{(n_R)}\} \\ = & \frac{1}{2} \text{Tr}\{[a_d^\dagger A_d^{(-)} - A_d^{(+)} a_d^\dagger] \rho(t) + \text{H.c.}\}, \end{aligned} \quad (3)$$

where  $\rho(t) = \sum_{n_R} \rho^{(n_R)}(t)$ .  $\rho(t)$  satisfies the usual *unconditional* master equation, which can be straightforwardly obtained in this context by summing up Eq. (2) over “ $n_R$ ”. Similar result as Eq. (3) can be obtained for  $I_L(t)$ , the current through the left junction.

Now we formulate the calculation of the output power spectrum. It is well known that the noise spectrum is a measure of the temporal correlation of the current. The temporal fluctuating currents through the left and right junctions, even in steady state, are not equal to each other. The circuit current, which is typically the measured quantity in most experiments, is a superposition of the left and right currents, i.e.,  $I(t) = aI_L(t) + bI_R(t)$ . Here the coefficients  $a$  and  $b$  satisfy  $a+b=1$ , and depend

on the junction capacitances of the detector [26]. Note that this capacitive geometry is *not* necessarily in accordance with the tunnel couplings. For very asymmetric tunnel couplings, the capacitive geometry can be quite symmetric. In what follows we shall see that this is in fact the setup we want to suggest.

In view of the charge conservation, i.e.,  $I_L = I_R + \dot{Q}$ , where  $Q$  is the charge on the central dots, we obtain  $I(t)I(0) = aI_L(t)I_L(0) + bI_R(t)I_R(0) - ab\dot{Q}(t)\dot{Q}(0)$ . Accordingly, the noise spectrum is a sum of three parts

$$S(\omega) = aS_L(\omega) + bS_R(\omega) - ab\omega^2 S_Q(\omega), \quad (4)$$

where  $S_{L/R}(\omega)$  is the noise spectrum of the current through the left (right) junction, and  $S_Q(\omega)$  characterizes the charge fluctuations on the central dots. For  $S_{L/R}(\omega)$ , it follows the MacDonald's formula

$$S_\alpha(\omega) = 2\omega \int_0^\infty dt \sin\omega t \frac{d}{dt} \langle n_\alpha^2(t) \rangle \quad (5)$$

where  $\langle n_\alpha^2(t) \rangle = \sum_{n_\alpha} n_\alpha^2 \text{Tr} \rho^{(n_\alpha)}(t) = \sum_{n_\alpha} n_\alpha^2 P(n_\alpha, t)$ . With the help of Eq. (2), we further obtain

$$\frac{d}{dt} \langle n_\alpha^2(t) \rangle = \text{Tr} [2\mathcal{J}_\alpha^{(-)} N^\alpha(t) + \mathcal{J}_\alpha^{(+)} \rho + \text{H.c.}], \quad (6)$$

where the *particle-number* matrix reads  $N_\alpha(t) \equiv \sum_{n_\alpha} n_\alpha \rho^{(n_\alpha)}(t)$ , and the superoperator means

$$\mathcal{J}_\alpha^{(\pm)}(\dots) = \frac{1}{2} [A_\mu^{(-)}(\dots) a_\mu^+ \pm a_\mu^+(\dots) A_\mu^{(+)}]. \quad (7)$$

In this last equation,  $\mu = c$  if  $\alpha = L$ ; and  $\mu = d$  if  $\alpha = R$ .

Following Ref. 24, it will be very convenient to work in the frequency domain. Inserting Eq. (6) into (5) we obtain

$$S_\alpha(\omega) = 2\omega \text{Im} [\text{Tr} \{ 2(\mathcal{J}_\alpha^{(-)} \tilde{N}^\alpha(\omega) + [\mathcal{J}_\alpha^{(-)} \tilde{N}^\alpha(-\omega)]^\dagger) + (\mathcal{J}_\alpha^{(+)} \tilde{\rho}(\omega) + [\mathcal{J}_\alpha^{(+)} \tilde{\rho}(-\omega)]^\dagger) \}], \quad (8)$$

where  $\tilde{N}^\alpha(\omega) = \int_0^\infty dt N^\alpha(t) e^{i\omega t}$ , and  $\tilde{\rho}(\omega) = \int_0^\infty dt \rho^{st} e^{i\omega t}$ . Note that  $\rho^{st}$  is the stationary state density matrix, which is time-independent. We thus have  $\tilde{\rho}(\omega) = i\rho^{st}/\omega$ . For  $N^\alpha(\omega)$ , it can be easily obtained by solving a set of algebraic equations after Fourier-transforming the equation of motion of  $N^\alpha(t)$ , as have been clearly described in Ref. 24.

Concerning the charge fluctuations on the central dots, we define the noise spectrum as

$$\begin{aligned} S_Q(\omega) &= \int_0^\infty d\tau \langle N(\tau)N + NN(\tau) \rangle e^{i\omega\tau} \\ &= 4\text{Re} \left[ \int_0^\infty d\tau S(\tau) e^{i\omega\tau} \right], \end{aligned} \quad (9)$$

where we have introduced  $S(\tau) = \langle N(\tau)N \rangle$ . More explicitly, it can be expressed as  $S(\tau) = \text{Tr} \text{Tr}_B [U^\dagger(\tau) N U(\tau) N \rho^{st} \rho_B]$ , where  $U(\tau) = e^{-iH\tau}$ , and  $N$  is the the electron number operator of the

central dots of the detector. Using the cyclic property under trace, we obtain  $S(\tau) = \text{Tr} [N\sigma(\tau)]$ , and  $\sigma(\tau) \equiv \text{Tr}_B [U(\tau) N \rho^{st} \rho_B U^\dagger(\tau)]$ . Obviously,  $\sigma(\tau)$  satisfies the same equation of the reduced density matrix  $\rho(\tau)$ . The only difference is the initial condition, for  $\sigma(\tau)$  which is  $\sigma(0) = N\rho^{st}$ . Similar to the above, from the equation of motion of  $\sigma(\tau)$ , its Fourier counterpart  $\tilde{\sigma}(\omega)$  can be straightforwardly carried out. Then, the charge fluctuation spectrum is obtained as  $S_Q(\omega) = 4\text{Re} \text{Tr} [N\tilde{\sigma}(\omega)]$ .

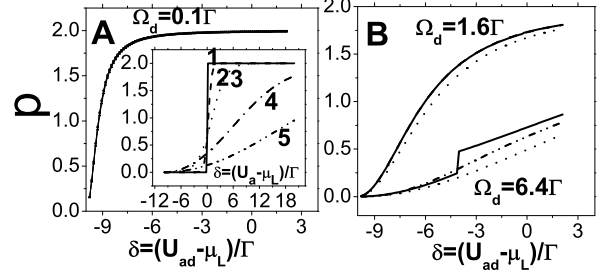


FIG. 2: Tolerance of (not low-enough) finite temperatures of the visibility,  $p = |\Delta I|/\bar{I} = 2|\Delta I|/(I_a + I_b)$ , for different inter-dot couplings of the DD detector: (A)  $\Omega_d/\Gamma = 0.1$ ; (B)  $\Omega_d/\Gamma = 1.6$  and  $6.4$ . As a comparison, the result of single-dot SET is plotted in the inset of (A), where  $U_a$  is the Coulomb interaction between the qubit electron in dot “a” and the transport electron in the central dot of SET. Results are illustrated for three temperatures for the DD detector,  $T/\Gamma = 0, 1.6$ , and  $12.8$  (corresponding to the solid, dot-dot-dashed, and dotted lines); while for five temperatures for the single-dot SET,  $T/\Gamma = 0, 0.4, 1.6, 6.4$  and  $12.8$  (labeled by “1”, “2”,  $\dots$ , and “5”). For the DD detector, the results are indistinguishable for small  $\Omega_d$  as shown in (A); the immunity against temperature will be weakened only for large  $\Omega_d$ , as shown in (B). In contrast, the visibility of the single-dot SET is affected by temperatures much more sensitively. In the whole calculations throughout the work, we assume that  $\Gamma_L = \Gamma$ , and use  $\Gamma$  as the energy unit. For the result shown in this figure, we chose  $\Gamma_R = \Gamma$ . Other parameters are adopted as:  $E_c = E_d = 0$ ,  $U_{ac} = U_{bc} = U_{bd} = 0$ ,  $\mu_L = 10\Gamma$ , and  $\mu_R = -10\Gamma$ .

Based upon the above formalism, we now investigate the readout characteristics of the DD detector. The first important quantity to characterize the detector is the *visibility*, which is defined by  $p = |\Delta I|/\bar{I} = 2|I_a - I_b|/(I_a + I_b)$ . In Fig. 2 we plot the visibility against the qubit-detector interaction strength “ $U_{ad}$ ”, by taking the temperature and the dot-dot coupling strength “ $\Omega_d$ ” of the DD detector as other comparative parameters. By comparing the results shown in Fig. 2(a) and (b), it is found that for smaller  $\Omega_d$  the visibility can more easily approach the ideal value of 2, by increasing the interaction strength “ $U_{ad}$ ”. In practice, controlling  $U_{ad}$  is difficult. However, engineering  $\Omega_d$  is relatively easy, which opens a way to

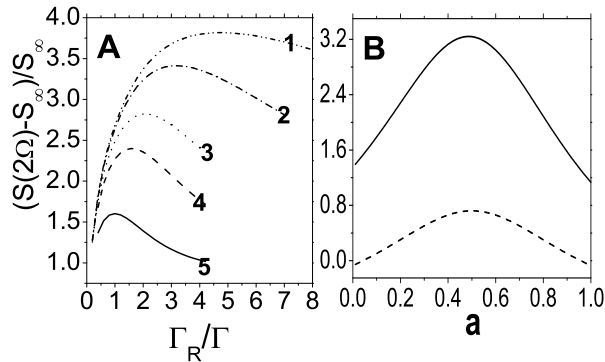


FIG. 3: Configuration symmetry dependence of the peak-to-pedestal ratio of the output power spectrum: (A)  $\Gamma_R$ -dependence, and (B) capacitive coupling dependence. Note that in (B) the parameter  $a$  characterizes the capacitive coupling symmetry (see the main text for its more detailed explanation). The major parameters are the same as in Fig. 2, except for the differences as follows: In present result, it is assumed that  $\Omega = \Omega_d = 0.2\Gamma$ , and the temperature  $T = 0$ . In (A), we assume a symmetric configuration of capacitive coupling, i.e.,  $a = 1/2$ ; and assume the Coulomb interaction strengths as (1)  $U_{ad}/\Gamma = 12$ , (2)  $U_{ad}/\Gamma = 6$ , (3)  $U_{ad}/\Gamma = 3$ , (4)  $U_{ad}/\Gamma = 2$ , and (5)  $U_{ad}/\Gamma = 1$ . In (B), in addition to the result depicted by the solid curve, which corresponds to the suggested location of the qubit nearby the *right dot* of the DD detector (as schematically shown in Fig. 1), we also plot the result by the dashed curve for the result of configuration with the qubit nearby the *left dot*. For the former configuration,  $U_{ac} = 0$  and  $U_{ad} = 6\Gamma$ ; while for the latter,  $U_{ad} = 0$  and  $U_{ac} = 6\Gamma$ . And for both configurations,  $\Gamma_R = 2\Gamma$  is commonly used.

enhance the visibility as revealed in Fig. 2. In this context, one should also notice another major advantage of the DD detector, say, its better tolerance to finite temperatures. From Fig. 2 we see that the finite temperature does not sensitively affect the operation of the DD detector under proper parametric conditions, particularly for small  $\Omega_d$  as shown in Fig. 2(a). Contrary to that, in the inset of Fig. 2(a), the result of single-dot detector is presented, of which the visibility sensitively depends on the temperature. All these features can be easily understood in terms of resonant tunnelling through the double dots and single dot, respectively.

In addition to the visibility, the quality of a quantum detector is well characterized by the signal-to-noise ratio, i.e., the *peak-to-pedestal* ratio of the output power spectrum. Not as in Ref. 21, where the capacitively asymmetric coupling model, i.e., with  $a = 0$  and  $b = 1$ , was taken into account, below we calculate the noise spectrum in general under arbitrary capacitive couplings. And in particular, the symmetric coupling, say,  $a = b = 1/2$ ,

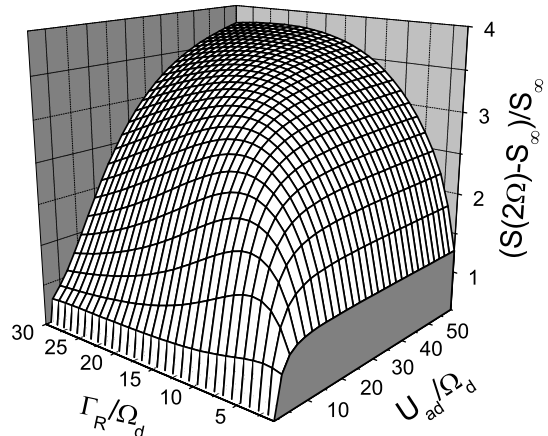


FIG. 4: 3D plot of the peak-to-pedestal ratio of the output power spectrum as a function of  $\Gamma_R$  and  $U_{ad}$ . Relevant parameters are the same as in Fig. 3A.

will be focused. Notably, from Fig. 3(a) we find that the peak-to-pedestal ratio is sensitively affected by the tunnel rate  $\Gamma_R$  of the right junction, where the measured qubit is placed nearby. This feature is in qualitative agreement with that found by Gurvitz *et al* [21], although a different definition of the signal-to-noise ratio was employed there.

In Fig. 3(b) we show the effect of the capacitive coupling symmetry. It is found that the signal-to-noise ratio will reach the maximum at the symmetric coupling, i.e., when  $a = 1/2$ . This is because the charge number fluctuation on the two dots of the detector has negative contribution to the noise spectrum, thus largely suppresses the background noise. As a consequence, the peak-to-pedestal ratio is enhanced for more symmetric coupling, and reaches the maximum at  $a = 1/2$ . In Fig. 3(b), the solid (dashed) curve corresponds to the result of the measured qubit next to the right (left) dot of the DD detector. This remarkable difference reflects another interesting symmetry effect of the setup configuration.

Notice that  $\Gamma_R$  and  $\Omega_d$  are two controllable parameters in practice. We thus re-plot the signal-to-noise ratio versus the scaled  $\Gamma_R$  and  $U_{ad}$  by  $\Omega_d$ , in order to gain the entire landscape more clearly as shown in Fig. 4. In this context, we remark that the peak-to-pedestal ratio of the DD detector can approach the upper limit of 4 of the *ideal* QPC detector [25], under proper parametric conditions as indicated by Fig. 4. This conclusion is in contrast to that by Gurvitz *et al* [6, 21]. There, it was concluded that both the single-dot and double-dots detectors are only *sensitive* measurement devices (i.e. with desirable visibility), but *cannot reach the effectiveness of an ideal QPC detector*. By tilting the tunnel coupling such that  $\Gamma_R \gg \Gamma_L$ , Gurvitz *et al* found that the signal-to-noise ratio can be considerably enhanced. However,

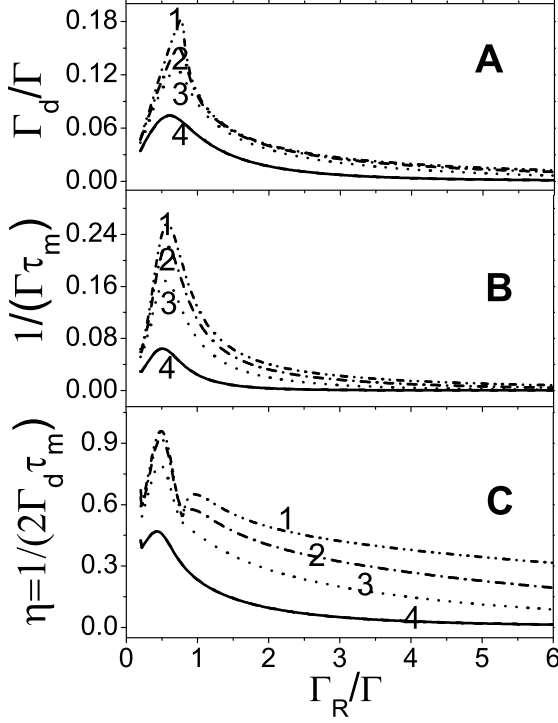


FIG. 5:  $\Gamma_R$ -dependence (i.e. asymmetric effect) of the dephasing rate (A), the measurement time (B), and the quantum measurement efficiency (C). Coulomb interaction strengths: (1)  $U_{ad}/\Gamma = 12$ , (2)  $U_{ad}/\Gamma = 6$ , (3)  $U_{ad}/\Gamma = 3$ , and (4)  $U_{ad}/\Gamma = 1$ . Other relevant parameters are referred to Fig. 3A.

their calculation was restricted to the *capacitively* asymmetric coupling model, i.e., with  $a = 0$  and  $b = 1$ . In this case, the upper limit of the signal-to-pedestal ratio is 2. Here, as clearly shown by Fig. 3(b), our calculation shows that under the symmetric condition  $a = b = 1/2$  the signal-to-pedestal ratio is maximal, and can in principle approach the value of 4, which is the upper limit of the ideal QPC detector [25].

### Dephasing and Measurement Times

In the orthodox Copenhagen postulate for quantum measurement, the measured wavefunction collapses onto one of the eigenstates of the observable *simultaneously*. In contrast to that, the wavefunction collapse in real device must need some time, i.e., the *measurement time*. On the other hand, during the collapsing process, dephasing between the superposed wavefunction components must take place *before* reading out the result. Therefore, the ratio of the dephasing time to the measurement time

is another deep criterion to characterize the *efficiency of quantum measurement*. In the following we carry out a quantitative analysis for the DD detector.

The analysis is also based on the “ $n$ ”-resolved master equation. Since in this context we are interested in the measurement-induced collapse of wavefunction, we consider the measurement of the idle state of the qubit. We thus set  $\Omega = 0$ , i.e., switch off the qubit state oscillation. Accordingly, all the mixing terms, i.e., those proportional to  $\Omega$ , disappear in Eq. (2). And the density matrix of the system factorizes into three independent groups. Furthermore, we restrict our analysis to zero temperature, and assume that  $E_i = 0$  for  $i = a, b, c$ , and  $d$ , and  $U_{ac} = U_{bc} = U_{bd} = 0$ . By Fourier transforming the resultant “ $n$ ”-resolved master equation, i.e., defining  $\rho(k, t) = \sum_{n_R} \rho^{(n_R)}(t) e^{in_R k}$ , we obtain

$$\dot{\rho}_{aa}^{00} = -\Gamma_L \rho_{aa}^{00} + \Gamma_R e^{ik} \rho_{aa}^{22} \quad (10a)$$

$$\dot{\rho}_{aa}^{11} = -i\Omega_d [\rho_{aa}^{21} - \rho_{aa}^{12}] + \Gamma_L \rho_{aa}^{00} \quad (10b)$$

$$\dot{\rho}_{aa}^{22} = -i\Omega_d [\rho_{aa}^{12} - \rho_{aa}^{21}] - \Gamma_R \rho_{aa}^{22} \quad (10c)$$

$$\dot{\rho}_{aa}^{12} = iU_{ad} \rho_{aa}^{12} - i\Omega_d [\rho_{aa}^{22} - \rho_{aa}^{11}] - \frac{1}{2} \Gamma_R \rho_{aa}^{12} \quad (10d)$$

$$\dot{\rho}_{bb}^{00} = -\Gamma_L \rho_{bb}^{00} + \Gamma_R e^{ik} \rho_{bb}^{22} \quad (10e)$$

$$\dot{\rho}_{bb}^{11} = -i\Omega_d [\rho_{bb}^{21} - \rho_{bb}^{12}] + \Gamma_L \rho_{bb}^{00} \quad (10f)$$

$$\dot{\rho}_{bb}^{22} = -i\Omega_d [\rho_{bb}^{12} - \rho_{bb}^{21}] - \Gamma_R \rho_{bb}^{22} \quad (10g)$$

$$\dot{\rho}_{bb}^{12} = -i\Omega_d [\rho_{bb}^{22} - \rho_{bb}^{11}] - \frac{1}{2} \Gamma_R \rho_{bb}^{12} \quad (10h)$$

$$\dot{\rho}_{ab}^{00} = -\Gamma_L \rho_{ab}^{00} + \Gamma_R e^{ik} \rho_{ab}^{22} \quad (10i)$$

$$\dot{\rho}_{ab}^{11} = -i\Omega_d [\rho_{ab}^{21} - \rho_{ab}^{12}] + \Gamma_L \rho_{ab}^{00} \quad (10j)$$

$$\dot{\rho}_{ab}^{22} = -iU_{ad} \rho_{ab}^{22} - i\Omega_d [\rho_{ab}^{12} - \rho_{ab}^{21}] - \Gamma_R \rho_{ab}^{22} \quad (10k)$$

$$\dot{\rho}_{ab}^{12} = -i\Omega_d [\rho_{ab}^{22} - \rho_{ab}^{11}] - \frac{1}{2} \Gamma_R \rho_{ab}^{12} \quad (10l)$$

$$\dot{\rho}_{ab}^{21} = -iU_{ad} \rho_{ab}^{21} - i\Omega_d [\rho_{ab}^{11} - \rho_{ab}^{22}] - \frac{1}{2} \Gamma_R \rho_{ab}^{21} \quad (10m)$$

We see that these equations split into three groups, i.e., (10a)-(10d), (10e)-(10h), and (10i)-(10m). Here, the density matrix elements  $\rho_{mn}^{ij} = \langle im | \rho | jn \rangle$ .  $|i\rangle$  and  $|j\rangle$  denote the occupation states of the DD detector, i.e.,  $|0\rangle \equiv |00\rangle$ ,  $|1\rangle \equiv |10\rangle$  and  $|2\rangle \equiv |01\rangle$ , respectively; while  $|m\rangle$  and  $|n\rangle$  denote the qubit states  $|a\rangle$  and  $|b\rangle$ .

We now consider the characteristic solutions of the the above three groups of equations, i.e., solutions proportional to  $e^{i\omega t}$ . Technically, for each group of Eqs. (10), we can obtain five eigenvalues. For small values of  $k \ll 1$ , from the former two groups of Eqs. (10) we obtain the smallest two eigenvalues  $\omega_j(k) = (k + \frac{1}{2} i f^j k^2) \Gamma^j$ , with  $j = a$  and  $b$ , respectively, which are most relevant to present analysis.  $\Gamma^j$  are the wave-packet’s group velocities, which actually correspond to the stationary currents  $I_j$ , with respect to the qubit in state  $|j\rangle$ ;  $f^j$  are the respective Fano factors. Explicitly, from Eqs. (10a)-(10h),

$\Gamma^j$  and  $f^j$  are obtained as

$$\Gamma^j = \frac{\Omega_d^2 \Gamma_R}{\left(\frac{\Gamma_R^2}{4} + U_j^2\right) + \Omega_d^2 \Gamma_R \left(\frac{1}{\Gamma_L} + \frac{2}{\Gamma_R}\right)} \equiv \frac{\Omega_d^2 \Gamma_R}{A_j} \quad (11)$$

$$f^j = 1 + \frac{2\Omega_d^2}{A_j} \left[ 2 - \frac{\Gamma_R^2 + \left(1 + \frac{\Gamma_R}{\Gamma_L}\right)\left(\frac{\Gamma_R^2}{4} + U_j^2 + 4\Omega_d^2\right)}{A_j} \right]. \quad (12)$$

Here, the Coulomb interaction energy  $U_a = U_{ad}$ , and  $U_b = 0$ , with the convention that the two dot-states of the DD detector are in resonance if the qubit is in state  $|b\rangle$ , and in off-resonance by an energy  $U_a = U_{ad}$  if the qubit is in state  $|a\rangle$ . Quantitatively, the measurement time can be defined as the required time for signal-to-noise ratio approaching unity. This condition leads to [3, 4]

$$t_m = \left( \frac{\sqrt{2f^a \Gamma^a} + \sqrt{2f^b \Gamma^b}}{\Gamma^a - \Gamma^b} \right)^2. \quad (13)$$

The dephasing time can be obtained by analyzing Eqs. (10i)-(10m) for  $k = 0$ . Similarly, solve the (five) eigenvalues  $\lambda_i$  of these equations, then determine the dephasing time in terms of  $t_d = \max[\text{Im}\lambda_i]^{-1}$ . Importantly, the quantum measurement efficiency is obtained via  $\eta = 1/(2\Gamma_d t_m)$ , where  $\Gamma_d = 1/t_d$ .

In Fig. 5 we plot the  $\Gamma_R$ -dependence of the measurement time, dephasing rate, and the quantum measurement efficiency. Notably, by either reducing  $\Gamma_R$  in the weak tunnel regime or increasing  $\Gamma_R$  in the (relatively) strong tunnel regime, the dephasing rate decreases. This can be understood as follows. In the former regime, the tunnel current is small. From the general point of view, dephasing is anyhow a result of the back-action of the current flowing in the measuring device. Therefore, the weak current will result in the small dephasing rate. On the other hand, in the latter regime, the duration time of the tunnel electron in the right dot of the DD detector is short. This will dephase the qubit state slowly. As a result, the strongest dephasing would take place at certain intermediate value of  $\Gamma_R$ , as shown in Fig. 5(a). The qualitative behavior of the measurement time, obviously, will follow the dephasing rate. This is plotted in Fig. 5(b).

Finally and interestingly, the quantum measurement efficiency, which is the ratio of the dephasing time and the measurement time, is shown in Fig. 5(c). Two remarks are worth being mentioned here: (i) The quantum measurement efficiency does not increase with  $\Gamma_R$ . This means that while the detector gains better signal-to-noise ratio by increasing  $\Gamma_R$ , however, the quantum measurement efficiency is *not* improved in accordance. This result is not surprising, since the quantum measurement efficiency is an alternative quantity to qualify the measurement process. That is, it describes how fast the measurement result can be read out in comparison with the dephasing of the qubit state under the influence of measurement. This result is in consistent with the usual statement that the single-electron-transistor is *not* an ideal detector. (ii) However, there exists indeed appropriate parametric conditions, see Fig. 5(c), under which the quantum measurement efficiency can *almost* approach unity.

## Conclusion

To summarize, we have presented a study for the quantum measurement characteristics of double-dot SET. Our study was based on a full analysis of the setup configuration symmetry, i.e., in terms of both tunneling strengths and capacitive couplings. We found that the DD detector can approach the signal-to-noise ratio of an ideal QPC detector, provided the symmetric capacitive coupling is taken into account. The measurement time, the measurement-induced dephasing time and the quantum measurement efficiency were calculated. It was found that the quantum measurement efficiency of the DD detector cannot reach unity, i.e., the value of ideal QPC detector, under the setup configuration that results in the optimal signal-to-noise ratio. However, in principle, it can approach unity under proper parametric conditions.

*Acknowledgments.* We sincerely thank the discussion from S. A. Gurvitz, which drew our attention on the double-dot detector and initiated the present work. Support from the National Natural Science Foundation of China (No. 60425412,60376037,90503013) and the Major State Basic Research Project of China (No. G001CB3095) is gratefully acknowledged.

---

[1] M. H. Devoret and R. J. Schoelkopf, Nature (London) **406**, 1039 (2000).  
 [2] A. Shnirman and G. Schön, Phys. Rev. B **57**, 15400 (1998).  
 [3] Y. Makhlin, G. Schön, and A. Shnirman, Rev. Mod. Phys. **73**, 357 (2001).  
 [4] I. L. Aleiner, N. S. Wingreen, and Y. Meir, Phys. Rev.

Lett. **79**, 3740 (1997).  
 [5] S. A. Gurvitz and Ya. S. Prager, Phys. Rev. B **53**, 15932 (1996).  
 [6] S. A. Gurvitz and G. P. Berman, Phys. Rev. B **72**, 073303 (2005).  
 [7] Hsi-Sheng Goan, G. J. Milburn, H. M. Wiseman, and He Bi Sun, Phys. Rev. B **63**, 125326 (2001).

- [8] E. Buks, R. Schuster, M. Heiblum, D. Mahalu, and V. Umansky, *Nature (London)* **391**, 871 (1998).
- [9] R. J. Schoelkopf, P. Wahlgren, A. A. Kozhevnikov, P. Delsing, and D. E. Prober, *Science* **280**, 1238 (1998).
- [10] M. Macucci, M. Gattobigio, and G. Iannaccone, *J. Appl. Phys.* **90**, 6428 (2001).
- [11] W. G. van derWiel, S. De Franceschi, J. M. Elzerman, T. Fujisawa, S. Tarucha, and L. P. Kouwenhoven, *Rev. Mod. Phys.* **75**, 1 (2003).
- [12] J. M. Elzerman, R. Hanson, L. H. Willems van Beveren, B. Witkamp, L. M. K. Vandersypen and L. P. Kouwenhoven, *Nature (London)* **430**, 431 (2004).
- [13] M. Xiao, I. Martin, E. Yablonovitch, and H. W. Jiang, *Nature (London)* **430**, 435 (2004).
- [14] S. Gustavsson, R. Leturcq, B. Simovic, R. Schleser, P. Studerus, T. Ihn, K. Ensslin, D. C. Driscoll, and A. C. Gossard, *Phys. Rev. B* **74**, 195305 (2006).
- [15] T. Fujisawa, T. Hayashi, R. Tomita, and Y. Hirayama, *Science* **312**, 1634 (2006).
- [16] M. Gattobigio, G. Iannaccone, and M. Macucci, *Phys. Rev. B* **65**, 115337 (2002).
- [17] R. Brenner, A. D. Greentree, and A. R. Hamilton, *Appl. Phys. Lett.* **83**, 4640 (2003).
- [18] R. Brenner, T. M. Buehler, and D. J. Reilly, *J. Appl. Phys.* **97**, 034501 (2005).
- [19] T. Tanamoto and X. Hu, *Phys. Rev. B* **69**, 115301 (2004).
- [20] Tamás Geszti and József Zsolt Bernád, *Phys. Rev. B* **73**, 235343 (2006).
- [21] T. Gilad and S. A. Gurvitz, *Phys. Rev. Lett.* **97**, 116806 (2006).
- [22] X. Q. Li, P. Cui, and Y. J. Yan, *Phys. Rev. Lett.* **94**, 066803 (2005).
- [23] X. Q. Li, J. Y. Luo, Y. G. Yang, P. Cui, and Y. J. Yan, *Phys. Rev. B* **71**, 205304 (2005).
- [24] J. Y. Luo, X. Q. Li, and Y. J. Yan, *cond-mat/0603163* (2006).
- [25] A. N. Korotkov, *Phys. Rev. B* **63**, 085312 (2001).
- [26] Ya. M. Blanter and M. Büttiker, *Phys. Rep.* **336**, 1 (2000).